

# Robust tracking and regulation control for mobile robots

W. E. Dixon, D. M. Dawson<sup>\*,†</sup>, E. Zergeroglu and F. Zhang

*Department of Electrical & Computer Engineering, Clemson University, Clemson, SC 29634-0915, U.S.A.*

## SUMMARY

This paper presents the design of a new, differentiable kinematic control law that utilizes a damped dynamic oscillator with a tunable frequency of oscillation to achieve global uniformly ultimately bounded tracking (i.e., the position/orientation tracking errors globally exponentially converge to a neighbourhood about zero that can be made arbitrarily small). In contrast to many of the previously developed kinematic tracking controllers, the proposed controller can be used for the regulation problem as well; hence, a unified framework is provided for both the tracking and the regulation problem. To compensate for uncertainty in the dynamic model, we illustrate how the kinematic controller can be used to design a robust nonlinear controller. Experimental results are presented to demonstrate the performance of the proposed controller. Copyright © 2000 John Wiley & Sons, Ltd.

KEY WORDS: robust; underactuated; nonholonomic; mobile robot

## 1. INTRODUCTION

The motion control problem of mechanical systems with non-holonomic constraints has been a heavily researched area due to both the challenging theoretical nature of the problem and its practical importance. One example of a non-holonomic system that has received a large amount of research activity is the wheeled mobile robot (WMR). In recent years, control researchers have targeted the problems of: (i) regulating the position and orientation of the WMR to an arbitrary setpoint, (ii) tracking a time-varying reference trajectory (which includes the *path following* problem as a special case [1]), and (iii) incorporating the effects of the dynamic model during the control design to enhance robustness. With regard to the control of non-holonomic systems, one of the technical hurdles often cited is that the regulation problem cannot be solved via a smooth, time-invariant state feedback law due to the implications of Brockett's condition [2]. To deal with this obstacle, some researchers have proposed controllers that utilize discontinuous control laws, piecewise continuous control laws, smooth time-varying control laws, or hybrid controllers to achieve setpoint regulation (see [3, 4], and the references therein for an in-depth review of the previous work). Specifically, in [5], Bloch *et al.* developed a piecewise continuous control structure for locally regulating several different types of non-holonomic systems to a setpoint. In

---

\* Corresponding address: D. M. Dawson, Department of Electrical & Computer Engineering, Clemson University, Clemson, SC 29634-0915, U.S.A.

† E-mail: ddawsson@ces.clemson.edu

Reference [6], Canudas de Wit and Sordalen constructed a piecewise smooth controller to exponentially stabilize a WMR to a setpoint; however, due to the control structure, the orientation of the WMR is not arbitrary. One of the first smooth, time-varying feedback controllers that could be utilized to asymptotically regulate a WMR to a desired setpoint was proposed by Samson in [4]. Smooth, time-varying controllers were also developed for other classes of non-holonomic systems in References [7–9]. More recently, in References [10, 11], global asymptotic feedback controllers for a general class of non-holonomic systems were developed, and hence, a control solution that could be used to stabilize a WMR to a desired posture was provided. In order to overcome the *slower*, asymptotic response of the previous smooth, time-varying controllers, Godhavn and Egeland [12] and McCloskey and Murray [3] constructed control laws that locally  $\rho$ -exponentially (as well globally asymptotically) stabilized classes of non-holonomic systems. Under the assumption of exact model knowledge, McCloskey and Murray [3] also illustrated how the dynamic model of a WMR could be included during the control design.

Several controllers have also been proposed for the reference robot tracking problem (i.e. the desired time-varying linear/angular velocity are specified). Specifically, in Reference [13], Kanayama *et al.* utilized a continuous feedback control law for a linearized kinematic model to obtain local asymptotic tracking; whereas, Walsh *et al.* [14] obtained local exponential stability results for a similar linearized model using a continuous, linear control law. In Reference [15], Jiang and Nijmeijer developed a global asymptotic tracking controller for a WMR; however, angular acceleration measurements were required. In Reference [16], Jiang and Nijmeijer provided semi-global and global asymptotic tracking solutions for the general chained system form, and hence, provided a solution for the WMR tracking problem that removed the need for angular acceleration measurements required in Reference [15]. In Reference [17], Escobar *et al.* illustrated how a field oriented induction motor controller can be redesigned to exponentially stabilize the non-holonomic double integrator control problem (e.g. Heisenberg flywheel); however, the controller exhibited singularities. To compensate for parametric uncertainty in the dynamic model, Dong and Huo [18] utilized the kinematic control proposed in Reference [11] to construct an adaptive control solution for a class of non-holonomic systems that yielded global asymptotic tracking. We also note that several researchers (see [1, 19], and the references within) have proposed various controllers for the path following problem.

From a review of the literature, it seems that we can make the following observations for the previously developed kinematic controllers: (i) the tracking controllers do not solve the regulation problem (i.e. restrictions on the reference model trajectory signals prohibit extension to the regulation problem), (ii) the stability results for the differentiable, kinematic controllers tend to be global asymptotic instead of global exponential, (iii) the heavy reliance of Barbalat's Lemma and its extensions during the kinematic stability analysis appear to prohibit the use of robust nonlinear controllers [20] for rejection of uncertainty associated with the dynamic model (i.e. the Lyapunov derivative is negative semi-definite in the system states as opposed to negative definite), and (iv) some of the kinematic controllers are not differentiable (e.g. see the kinematic controller developed in Reference [3]), and unfortunately, the standard backstepping procedure, often used for incorporating the mechanical dynamics, requires that the kinematic controller be differentiable (see the discussion in Reference [3]). In an attempt to address the above issues, we present the design of a new, differentiable kinematic control law that achieves global uniformly ultimately bounded (GUUB) tracking control for a WMR. That is, the position and orientation tracking errors globally exponentially converge to a neighbourhood about zero that can be made

arbitrarily small. Since the kinematic tracking controller does not restrict the reference model in any way, the proposed kinematic controller can also be used for the regulation problem; hence, we present a unified control framework for both the tracking and regulation problem. Moreover, since the proposed kinematic controller is differentiable, we illustrate how standard backstepping techniques can be used to design a nonlinear robust controller that compensates for uncertainty associated with the dynamic model (i.e. parameter uncertainty and additive bounded disturbances). We note that the proposed kinematic controller does not utilize explicit sinusoidal terms in the feedback controller; rather, a damped dynamic oscillator with a tunable frequency of oscillation is constructed. Roughly speaking, the frequency of oscillation is used as an auxiliary control input to cancel odious terms during the Lyapunov analysis. It should be noted that the proposed solution to the kinematic problem is crucial for developing the proposed robust controller for the dynamic model (i.e. the Lyapunov derivative is negative definite in the system states as opposed to negative semi-definite).

The paper is organized as follows. In Section 2, we transform the kinematic model of a WMR into a form which facilitates the subsequent control development. In Section 3, we present the control development and corresponding stability analysis to illustrate GUUB tracking for the kinematic model. In Section 4, we develop the dynamic model for a WMR which facilitates the subsequent control development and stability analysis. In Section 5, we reconfigure the controller to illustrate GUUB tracking for the dynamic model. Experimental verification of the controller's performance is presented in Section 6. In Section 7, we present some concluding remarks.

## 2. KINEMATIC PROBLEM FORMULATION

### 2.1. WMR kinematic model

The kinematic model for the so-called kinematic wheel under the non-holonomic constraint of *pure rolling* and *non-slipping* is given as follows [3]:

$$\dot{q} = S(q)v \quad (1)$$

where  $q(t), \dot{q}(t) \in \mathfrak{R}^3$  are defined as

$$q = [x_c \ y_c \ \theta]^T, \quad \dot{q} = [\dot{x}_c \ \dot{y}_c \ \dot{\theta}]^T \quad (2)$$

$x_c(t), y_c(t)$ , and  $\theta(t) \in \mathfrak{R}^1$  denote the linear position and orientation, respectively, of the centre of mass (COM) of the WMR,  $\dot{x}_c(t), \dot{y}_c(t)$  denote the Cartesian components of the linear velocity of the COM,  $\dot{\theta}(t) \in \mathfrak{R}^1$  denotes the angular velocity of the COM, the matrix  $S(q) \in \mathfrak{R}^{3 \times 2}$  is defined as follows:

$$S(q) = \begin{bmatrix} \cos \theta & 0 \\ \sin \theta & 0 \\ 0 & 1 \end{bmatrix} \quad (3)$$

and the velocity vector  $v(t) \in \mathfrak{R}^2$  is defined as

$$v = [v_1 \ v_2]^T = [v_1 \ \dot{\theta}]^T \quad (4)$$

with  $v_1(t) \in \mathfrak{R}^1$  denoting the linear velocity of the COM of the WMR.

## 2.2. Control objective

As defined in previous work (e.g. see [13, 15]), the reference trajectory for the WMR is generated via a reference robot which moves according to the following dynamic trajectory:

$$\dot{q}_r = S(q_r)v_r \quad (5)$$

where  $S(\cdot)$  was defined in (3),  $q_r(t) = [x_{rc}(t) \ y_{rc}(t) \ \theta_r(t)]^T \in \mathfrak{R}^3$  denotes the desired time-varying position and orientation trajectory, and  $v_r(t) = [v_{r1}(t) \ v_{r2}(t)]^T \in \mathfrak{R}^2$  denotes the reference time-varying linear and angular velocity. With regard to (5), it is assumed that the signal  $v_r(t)$  is constructed to produce the desired motion and that  $v_r(t)$ ,  $\dot{v}_r(t)$ ,  $q_r(t)$ , and  $\dot{q}_r(t)$  are bounded for all time.

To facilitate the subsequent control synthesis and the corresponding stability proof, we define the following transformation:

$$\begin{bmatrix} w \\ z_1 \\ z_2 \end{bmatrix} = \begin{bmatrix} -\tilde{\theta} \cos \theta + 2 \sin \theta & -\tilde{\theta} \sin \theta - 2 \cos \theta & 0 \\ 0 & 0 & 1 \\ \cos \theta & \sin \theta & 0 \end{bmatrix} \begin{bmatrix} \tilde{x} \\ \tilde{y} \\ \tilde{\theta} \end{bmatrix} \quad (6)$$

where  $w(t) \in \mathfrak{R}^1$  and  $z(t) = [z_1(t) \ z_2(t)]^T \in \mathfrak{R}^2$  are auxiliary tracking error variables, and  $\tilde{x}(t)$ ,  $\tilde{y}(t)$ ,  $\tilde{\theta}(t) \in \mathfrak{R}^1$  denote the difference between the actual Cartesian position and orientation of the COM and the reference position and orientation of the COM as follows:

$$\tilde{x} = x_c - x_{rc}, \quad \tilde{y} = y_c - y_{rc}, \quad \tilde{\theta} = \theta - \theta_r. \quad (7)$$

After taking the time derivative of (6) and using (1)–(5), and (7), we can rewrite the tracking error dynamics in terms of the auxiliary variables defined in (6) as follows:

$$\begin{aligned} \dot{w} &= u^T J^T z + f \\ \dot{z} &= u \end{aligned} \quad (8)$$

where  $J \in \mathfrak{R}^{2 \times 2}$  is defined as

$$J = \begin{bmatrix} 0 & -1 \\ 1 & 0 \end{bmatrix} \quad (9)$$

$f(z, v_r, t) \in \mathfrak{R}^1$  is defined as

$$f = 2(v_{r2}z_2 - v_{r1} \sin z_1) \quad (10)$$

and the auxiliary variable  $u(t) = [u_1(t) \ u_2(t)]^T \in \mathfrak{R}^2$  is defined in terms of the WMR position and orientation, the WMR linear velocities, and the desired trajectory as follows:

$$u = T^{-1}v - \begin{bmatrix} v_{r2} \\ v_{r1} \cos \tilde{\theta} \end{bmatrix} \quad v = Tu + \begin{bmatrix} v_{r1} \cos \tilde{\theta} + v_{r2}(\tilde{x} \sin \theta - \tilde{y} \cos \theta) \\ v_{r2} \end{bmatrix} \quad (11)$$

where the matrix  $T \in \mathfrak{R}^{2 \times 2}$  is defined as follows:

$$T = \begin{bmatrix} (\tilde{x} \sin \theta - \tilde{y} \cos \theta) & 1 \\ 1 & 0 \end{bmatrix}. \quad (12)$$

### 3. KINEMATIC CONTROL DEVELOPMENT

Our control objective is to design a kinematic controller for the transformed WMR kinematic model given by (8). To facilitate the subsequent control development, we define an auxiliary error signal  $\tilde{z}(t) \in \mathfrak{R}^2$  as the difference between the subsequently designed auxiliary signal  $z_d(t) \in \mathfrak{R}^2$  and the transformed variable  $z(t)$ , defined in (6), as follows:

$$\tilde{z} = z_d - z \quad (13)$$

#### 3.1. Control formulation

Based on the kinematic equations given in (8) and the subsequent stability analysis, we design the auxiliary signal  $u(t)$  as follows:

$$u = u_a - k_2 z \quad (14)$$

where the auxiliary control term  $u_a(t) \in \mathfrak{R}^2$  is defined as

$$u_a = \left( \frac{k_1 w + f}{\delta_d^2} \right) J z_d + \Omega_1 z_d \quad (15)$$

the auxiliary signal  $z_d(t)$  is defined by the following oscillator-like relationship:

$$\dot{z}_d = \frac{\dot{\delta}_d}{\delta_d} z_d + \left( \frac{k_1 w + f}{\delta_d^2} + w \Omega_1 \right) J z_d, \quad z_d^T(0) z_d(0) = \delta_d^2(0) \quad (16)$$

the auxiliary terms  $\Omega_1(w, z, v_r, t) \in \mathfrak{R}^1$  and  $\delta_d(t) \in \mathfrak{R}^1$  are defined as

$$\Omega_1 = k_2 + \frac{\dot{\delta}_d}{\delta_d} + w \left( \frac{k_1 w + f}{\delta_d^2} \right) \quad (17)$$

and

$$\delta_d = \alpha_0 \exp(-\alpha_1 t) + \varepsilon_1 \quad (18)$$

respectively,  $k_1, k_2, \alpha_0, \alpha_1, \varepsilon_1 \in \mathfrak{R}^1$  are positive, constant control gains, and  $f(z, v_r, t)$  was defined in (10).

#### Remark 1

Motivation for the structure of (16) is obtained by taking the time derivative of  $z_d^T z_d$  as follows:

$$\frac{d}{dt} (z_d^T z_d) = 2 z_d^T \dot{z}_d = 2 z_d^T \left( \frac{\dot{\delta}_d}{\delta_d} z_d + \left( \frac{k_1 w + f}{\delta_d^2} + w \Omega_1 \right) J z_d \right) \quad (19)$$

where (16) has been utilized. After noting that the matrix  $J$  of (9) is skew symmetric, we can rewrite (19) as follows:

$$\frac{d}{dt} (z_d^T z_d) = 2 \frac{\dot{\delta}_d}{\delta_d} z_d^T z_d. \quad (20)$$

As result of the selection of the initial conditions given in (16), it is easy to verify that

$$z_d^T z_d = \|z_d\|^2 = \delta_d^2 \quad (21)$$

is a unique solution to the differential equation given in (20). The relationship given by (21) will be used during the subsequent error system development and stability analysis.

*Remark 2*

Note that the exponential term in (18) is not necessary for the subsequent stability analysis. That is, if  $\alpha_0$  is selected as  $\alpha_0 = 0$  then the subsequent stability proof is still valid. The motivation for selecting  $\alpha_0 \neq 0$  is to provide the designer with increased flexibility with regard to ensuring that the control effort is maintained at a reasonable magnitude. Specifically, for the case of large initial tracking error, the magnitude of the control could possibly be reduced through the selection of  $\alpha_0$ .

*Remark 3*

Note that based on (10), we can place an upper bound on  $f(z, v_r, t)$  as follows:

$$f \leq 4\|v_r\|\|z\| \quad (22)$$

where we utilized the fact that

$$|\sin(z_1)| \leq |z_1|; \quad (23)$$

furthermore, we can utilize (13) to upper bound  $f(z, v_r, t)$  as follows:

$$f \leq 4\|v_r\|(\|z_d\| + \|\tilde{z}\|). \quad (24)$$

### 3.2. Error system development

To facilitate the closed-loop error system development, we substitute (14) for  $u(t)$ , add and subtract  $u_a^T J z_d$  to the resulting expression, utilize (13), and exploit the skew symmetry of  $J$  defined in (9) to rewrite the dynamics for  $w(t)$ , given by (8), as follows:

$$\dot{w} = u_a^T J \tilde{z} - u_a^T J z_d + f \quad (25)$$

where the fact that  $J^T = -J$  was utilized. Finally, by substituting (15) for only the second occurrence of  $u_a(t)$  in (25) and then utilizing the equality given by (21), the skew symmetry of  $J$  defined in (9), and the fact that  $J^T J = I_2$  (note that  $I_2$  denotes the standard  $2 \times 2$  identity matrix), we can obtain the final expression for the closed-loop error system for  $w(t)$  as follows:

$$\dot{w} = u_a^T J \tilde{z} - k_1 w. \quad (26)$$

To determine the closed-loop error system for  $\tilde{z}(t)$ , we take the time derivative of (13), substitute (16) for  $\dot{z}_d(t)$ , and then substitute (8) for  $\dot{z}(t)$  to obtain

$$\dot{\tilde{z}} = \frac{\dot{\delta}_d}{\delta_d} z_d + \left( \frac{k_1 w + f}{\delta_d^2} + w \Omega_1 \right) J z_d - u \quad (27)$$

After substituting (14) for  $u(t)$ , and then substituting (15) for  $u_a(t)$  in the resulting expression, we can rewrite the expression given by (27) as follows:

$$\dot{\tilde{z}} = \frac{\dot{\delta}_d}{\delta_d} z_d + w \Omega_1 J z_d - \Omega_1 z_d + k_2 z. \quad (28)$$

After substituting (17) for only the second occurrence of  $\Omega_1(t)$  in (28) and using the fact that  $JJ = -I_2$ , we can cancel common terms and rearrange the resulting expression to obtain

$$\dot{\tilde{z}} = -k_2\tilde{z} + wJ \left[ \left( \frac{k_1w + f}{\delta_d^2} \right) Jz_d + \Omega_1z_d \right] \tag{29}$$

where (13) has been utilized. Finally, since the bracketed term in (29) is equal to  $u_a(t)$  defined in (15), we can obtain the final expression for the closed-loop error system for  $\dot{\tilde{z}}(t)$  as follows:

$$\dot{\tilde{z}} = -k_2\tilde{z} + wJu_a. \tag{30}$$

3.3. Stability analysis

Theorem 1

Provided the desired trajectory (i.e.  $v_r(t)$ ,  $\dot{v}_r(t)$ ,  $q_r(t)$ , and  $\dot{q}_r(t)$ ) is selected to be bounded for all time  $t \geq 0$ , the kinematic control law given in (14)–(18) ensures the position and orientation tracking errors defined in (7) are GUUB in the sense that

$$|\tilde{x}(t)|, |\tilde{y}(t)|, |\tilde{\theta}(t)| \leq \beta_0 \exp(-\gamma_0 t) + \beta_1 \varepsilon_1 \tag{31}$$

where  $\varepsilon_1$  was defined in (18), and  $\beta_0$ ,  $\beta_1$ , and  $\gamma_0 \in \mathfrak{R}^1$  are some positive constants.

*Proof.* To prove Theorem 1, we define the following non-negative, scalar function denoted by  $V(w(t), \tilde{z}(t)) \in \mathfrak{R}^1$  as follows:

$$V = \frac{1}{2} w^2 + \frac{1}{2} \tilde{z}^T \tilde{z} \tag{32}$$

After taking the time derivative of (32) and making the appropriate substitutions from (26) and (30), we obtain the following expression:

$$\dot{V} = w[-k_1w + u_a^T J \tilde{z}] + \tilde{z}^T [-k_2\tilde{z} + wJu_a] \tag{33}$$

After utilizing the fact that  $J^T = -J$  and cancelling common terms, we obtain the following expression:

$$\dot{V} = -k_1w^2 - k_2\tilde{z}^T \tilde{z}. \tag{34}$$

Next, we can use (32) to upper bound  $\dot{V}(w(t), \tilde{z}(t))$  as follows:

$$\dot{V} \leq -2 \min(k_1, k_2)V. \tag{35}$$

Standard arguments can now be employed to solve the differential inequality given in (35) as shown below

$$V \leq \exp(-2 \min(k_1, k_2)t)V(w(0), \tilde{z}(0)). \tag{36}$$

Finally, we can utilize (32) to rewrite the inequality given by (36) as

$$\|\Psi_1(w(t), \tilde{z}(t))\| \leq \exp(-\min(k_1, k_2)t) \|\Psi_1(w(0), \tilde{z}(0))\| \quad (37)$$

where the vector  $\Psi_1(w(t), \tilde{z}(t)) \in \mathfrak{R}^3$  is defined as

$$\Psi_1 = [w \ \tilde{z}^T]^T. \quad (38)$$

Based on (37) and (38), it is straightforward to see that  $w(t), \tilde{z}(t) \in \mathcal{L}_\infty$ . After utilizing (13), (21), and the fact that  $\tilde{z}(t), \delta_d(t) \in \mathcal{L}_\infty$ , we can conclude that  $z(t), z_d(t) \in \mathcal{L}_\infty$ . Based on these facts, we can now use (14)–(18), and (21) to show that  $u_a(t), \dot{z}_d(t), \Omega_1(t), u(t) \in \mathcal{L}_\infty$ . Now, in order to illustrate that the Cartesian position and orientation signals defined in (1) are bounded, we calculate the inverse transformation of (6) as follows:

$$\begin{bmatrix} \tilde{x} \\ \tilde{y} \\ \tilde{\theta} \end{bmatrix} = \begin{bmatrix} 0 & \frac{1}{2}(\tilde{\theta} \sin \theta + 2 \cos \theta) & -\frac{1}{2} \sin \theta \\ 0 & -\frac{1}{2}(\tilde{\theta} \cos \theta + 2 \sin \theta) & -\frac{1}{2} \cos \theta \\ 1 & 0 & 0 \end{bmatrix} \begin{bmatrix} z_1 \\ z_2 \\ w \end{bmatrix}. \quad (39)$$

Since  $z(t) \in \mathcal{L}_\infty$ , it is clear from (7) and (39) that  $\tilde{\theta}(t), \theta(t) \in \mathcal{L}_\infty$ . Furthermore, from (7), (39), and the fact that  $w(t), z(t), \tilde{\theta}(t) \in \mathcal{L}_\infty$ , we can conclude that  $\tilde{x}(t), \tilde{y}(t), x_c(t), y_c(t) \in \mathcal{L}_\infty$ . We can utilize (11), the assumption that the desired trajectory is differentiable, and the fact that  $\theta(t), u(t), \tilde{x}(t), \tilde{y}(t) \in \mathcal{L}_\infty$ , to show that  $v(t) \in \mathcal{L}_\infty$ ; therefore, it follows from (1)–(4) that  $\dot{\theta}(t), \dot{x}_c(t), \dot{y}_c(t) \in \mathcal{L}_\infty$ . We can now employ standard signal chasing arguments to conclude that all of the remaining signals in the control and the system remain bounded during closed-loop operation.

In order to prove (31), we first show that  $z(t)$  defined in (6) is GUUB by applying the triangle inequality to (13) to obtain the following bound for  $z(t)$

$$\|z\| \leq \|\tilde{z}\| + \|z_d\| \leq \exp(-\min(k_1, k_2)t) \|\Psi_1(w(0), \tilde{z}(0))\| + \alpha_0 \exp(-\alpha_1 t) + \varepsilon_1 \quad (40)$$

where (18), (21), (37) and (38) have been utilized. The result given in (31) can now be directly obtained from (37), (38), (39), and (40).  $\square$

#### 4. DYNAMIC PROBLEM FORMULATION

Practical issues (e.g. robustness to uncertainty in the dynamic model) provide motivation to include the dynamic model as part of the overall control problem. As a result of this motivation, we describe the dynamic model of the WMR and then demonstrate how the integrator backstepping technique along with simple modifications to the proposed kinematic controller can be utilized to develop a robust controller for the WMR dynamic model.

##### 4.1. WMR dynamic model

The dynamic model for a WMR similar to the kinematic wheel can be easily expressed in the following form:

$$M\dot{v} + F(v) + T_d = B\tau \quad (41)$$

where  $\dot{v}(t) \in \mathfrak{R}^2$  denotes the time derivative of  $v(t)$  defined in (4),  $M \in \mathfrak{R}^{2 \times 2}$  represents the constant inertia matrix,  $F(v) \in \mathfrak{R}^2$  represents the friction effects,  $T_d(t) \in \mathfrak{R}^2$  represents a vector of unknown, bounded disturbances,  $\tau(t) \in \mathfrak{R}^2$  represents the torque input vector, and  $B \in \mathfrak{R}^{2 \times 2}$  represents an input matrix that governs torque transmission.



To facilitate the subsequent control design, we premultiply (41) by  $T^T$  and substitute (11) and (12) for  $v(t)$  to obtain the following convenient dynamic model:

$$\bar{M}\dot{u} + \bar{N} = \bar{B}\tau \quad (42)$$

where  $\bar{M} = T^TMT$ ,  $\bar{N} = T^T(M\dot{T}u + F(v) + T_d + M\Pi)$ ,  $\bar{B} = T^TB$ , and  $\Pi \in \mathfrak{R}^2$  is given by

$$\Pi = \begin{bmatrix} \dot{v}_{r1} \cos \tilde{\theta} - v_{r1} \dot{\tilde{\theta}} \sin \tilde{\theta} + \dot{v}_{r2}(\tilde{x} \sin \theta - \tilde{y} \cos \theta) + v_{r2}(\tilde{x}\dot{\theta} \cos \theta + \dot{\tilde{x}} \sin \theta + \tilde{y}\dot{\theta} \sin \theta - \dot{\tilde{y}} \cos \theta) \\ \dot{v}_{r2} \end{bmatrix} \quad (43)$$

The dynamic equation of (42) exhibits the following property which will be employed during the subsequent control development and stability analysis.

#### Property 1

The transformed inertia matrix  $\bar{M}$  is symmetric, positive definite, and satisfies the following inequalities [21]:

$$m_1 \|\xi\|^2 \leq \xi^T \bar{M} \xi \leq m_2(z, w) \|\xi\|^2 \quad \forall \xi \in \mathfrak{R}^2 \quad (44)$$

where  $m_1$  is a known positive constant,  $m_2(z, w) \in \mathfrak{R}^1$  is a known, positive bounding function which is assumed to be bounded provided its arguments are bounded, and  $\|\cdot\|$  is the standard Euclidean norm. Based on the fact that  $\bar{M}$  is symmetric and positive definite, we can use (44) to show that the inverse of  $\bar{M}$  satisfies the following inequality:

$$\frac{1}{m_2(z, w)} \|\xi\|^2 \leq \xi^T \bar{M}^{-1} \xi \leq \frac{1}{m_1} \|\xi\|^2 \quad \forall \xi \in \mathfrak{R}^2 \quad (45)$$

## 5. DYNAMIC CONTROL DEVELOPMENT

### 5.1. Control formulation

Based on the desire to incorporate the dynamic model in the control design, we design a robust<sup>‡</sup> controller for the dynamic model given by (42). To this end, we design the control torque input  $\tau(t)$  as follows:

$$\tau = (\bar{B})^{-1}(\hat{\kappa} + k_3 m_2(z, w)\eta + v_R) \quad (46)$$

where  $\eta(t) \in \mathfrak{R}^2$  denotes the kinematic tracking error signal defined as follows:

$$\eta = u_d - u \quad (47)$$

$u_d(t) \in \mathfrak{R}^2$  denotes the desired kinematic control signal

$$u_d = u_a - k_2 z \quad (48)$$

$u_a(t)$  was defined in (15),  $m_2(z, w)$  was defined in (44),  $\hat{\kappa}(\eta, w, z_d, z, t) \in \mathfrak{R}^2$  is a best guess estimate of the dynamic term denoted by  $\kappa(\eta, w, z_d, z, t) \in \mathfrak{R}^2$  which is explicitly defined as

$$\kappa = \bar{M}\dot{u}_d + \bar{N} \quad (49)$$

<sup>‡</sup> Roughly speaking, the controller will be designed to reject parametric uncertainty and additive bounded disturbances.

the auxiliary robust control term  $v_R(\eta, w, z_d, z, t) \in \mathfrak{R}^2$  is defined as

$$v_R = \frac{m_2(z, w)\eta\rho^2}{\|\eta\|\rho + \varepsilon_2} \quad (50)$$

$k_3, \varepsilon_2 \in \mathfrak{R}^1$  are positive, constant control gains, and the bounding function  $\rho(\eta, w, z_d, z, t) \in \mathfrak{R}^1$  is constructed to satisfy the following inequality:

$$\rho \geq \|\bar{M}^{-1}(\kappa - \hat{\kappa} + \bar{M}Jz_w + \bar{M}\hat{z})\|. \quad (51)$$

To facilitate the construction of  $\rho(\cdot)$ , the closed-form expression for  $\dot{u}_d(t)$  used in (49) is calculated in Appendix A.

*Remark 4*

One method for constructing  $\hat{\kappa}(\cdot)$  and  $\rho(\cdot)$  used in (46) and (50) is to note that part of  $\kappa(\cdot)$  can be linear parameterized as follows:

$$\bar{M}\dot{u}_d + T^T(M\dot{T}u + F(v) + M\Pi) = Yd\phi \quad (52)$$

where  $\phi \in \mathfrak{R}^p$  contains the unknown constant system parameters, and the regression matrix  $Y_d(\eta, w, z_d, z, t) \in \mathfrak{R}^{2 \times p}$  contains known functions. Hence,  $\hat{\kappa}(\cdot)$  could be constructed as follows:

$$\hat{\kappa}(\cdot) = Yd\phi \quad (53)$$

where  $\phi(t) \in \mathfrak{R}^p$  denotes the constant, best-guess parameter estimate vector. To satisfy (51), it would be an easy matter to use upper and lower bounds of the maximum parameter error and the additive bounded disturbance to construct  $\rho(\cdot)$  as follows:

$$\rho \geq \|\bar{M}^{-1}(Y_d\tilde{\phi} + \bar{T}_d + \bar{M}Jz_w + \bar{M}\hat{z})\| \quad (54)$$

where  $\tilde{\phi}(t) \in \mathfrak{R}^p$  is defined as shown below

$$\tilde{\phi} = \phi - \hat{\phi}. \quad (55)$$

### 5.2. Error system development

To facilitate the closed-loop error system development, we inject the auxiliary control input  $u_d(t)$  into the open-loop dynamics of  $w(t)$  given by (8) by adding and subtracting the term  $u_d^T Jz$  to the right-hand side of (8) and utilizing (47) to obtain the following expression:

$$\dot{w} = -u_d^T Jz + \eta^T Jz + f. \quad (56)$$

After substituting (48) for  $u_d(t)$ , adding and subtracting  $u_a^T Jz_d$  to the resulting expression, utilizing (13), and exploiting the skew symmetry of  $J$  defined in (9), we can rewrite the dynamics for  $w(t)$  as follows

$$\dot{w} = -u_a^T Jz_d + u_a^T J\tilde{z} + \eta^T Jz + f. \quad (57)$$

By utilizing the same techniques illustrated in the kinematic control development, we can obtain the final expression for the closed-loop error system for  $w(t)$  as follows:

$$\dot{w} = -k_1 w + u_a^T J\tilde{z} + \eta^T Jz. \quad (58)$$

To determine the closed-loop error system for  $\tilde{z}(t)$ , we take the time derivative of (13), substitute (16) for  $\dot{z}_d(t)$ , and then substitute (8) for  $\dot{z}(t)$  to obtain

$$\dot{\tilde{z}} = \frac{\dot{\delta}_d}{\delta_d} z_d + \left( \frac{k_1 w + f}{\delta_d^2} + w\Omega_1 \right) J z_d + \eta - u_d \tag{59}$$

where the auxiliary control input  $u_d(t)$  was injected by adding and subtracting  $u_d(t)$  to the right-hand side of (59), and (47) was utilized. After substituting (48) for  $u_d(t)$  and then substituting (15) for  $u_a(t)$  in the resulting expression, we can rewrite (59) as follows:

$$\dot{\tilde{z}} = \frac{\dot{\delta}_d}{\delta_d} z_d + w\Omega_1 J z_d - \Omega_1 z_d + k_2 z + \eta. \tag{60}$$

Based on the same procedure as described in the kinematic control development, we can now obtain the final expression for the closed-loop error system for  $\dot{\tilde{z}}(t)$  as shown below

$$\dot{\tilde{z}} = -k_2 \tilde{z} + w J u_a + \eta. \tag{61}$$

In order to develop the closed-loop error system for  $\eta(t)$ , we take the time derivative of (47), substitute for  $\dot{u}(t)$  from (42), and then rearrange the resulting expression to obtain the following expression:

$$\dot{\eta} = \bar{M}^{-1}(\kappa - \bar{B}\tau) \tag{62}$$

where (49) has been utilized. After substituting for the control torque input  $\tau(t)$  defined in (46), we obtain the closed-loop error system for  $\eta(t)$  as follows:

$$\dot{\eta} = -k_3 m_2(z, w) \bar{M}^{-1} \eta + \bar{M}^{-1}(\kappa - \hat{\kappa} + \bar{M} J z w + \bar{M} \tilde{z}) - \bar{M}^{-1} v_R - J z w - \tilde{z} \tag{63}$$

where  $J z w + \tilde{z}$  has been added and subtracted to the right-hand side of (63) to facilitate the following stability analysis.

### 5.3. Stability analysis

#### Theorem 2

Provided the desired trajectory (i.e.  $v_r(t)$ ,  $\dot{v}_r(t)$ ,  $q_r(t)$ , and  $\dot{q}_r(t)$ ) is selected to be bounded for all time  $t \geq 0$ , the dynamic control law given in (15)–(18), (46)–(50) ensures the position and orientation tracking errors defined in (7) are GUUB in the sense that

$$|\tilde{x}(t)|, |\tilde{y}(t)|, |\tilde{\theta}(t)| \leq \sqrt{\beta_2 \exp(-\gamma_1 t) + \varepsilon_2 \beta_3} + \beta_4 \exp(-\gamma_2 t) + \beta_5 \varepsilon_1 \tag{64}$$

where  $\varepsilon_1$  and  $\varepsilon_2$  are defined in (18) and (50), respectively, and  $\beta_2, \beta_3, \beta_4, \beta_5, \gamma_1$ , and  $\gamma_2 \in \mathfrak{R}^1$  are some positive constants.

*Proof.* To prove Theorem 2, we define the following non-negative, scalar function denoted by  $V_2(w(t), \tilde{z}(t), \eta(t)) \in \mathfrak{R}^1$  as follows:

$$V_2 = \frac{1}{2} w^2 + \frac{1}{2} \tilde{z}^T \tilde{z} + \frac{1}{2} \eta^T \eta. \tag{65}$$

After taking the time derivative of (65) and making the appropriate substitutions from (58), (61), and (63), we obtain the following expression:

$$\begin{aligned} \dot{V}_2 = & w[-k_1 w + u_a^T J \tilde{z} + \eta^T J z] + \tilde{z}^T[-k_2 \tilde{z} + w J u_a + \eta] \\ & + \eta^T[-k_3 m_2(z, w) \bar{M}^{-1} \eta + \bar{M}^{-1}(\kappa - \hat{\kappa} + \bar{M} J z w + \bar{M} \tilde{z}) - \bar{M}^{-1} v_R - J z w - \tilde{z}]. \end{aligned} \quad (66)$$

After cancelling common terms, utilizing (51), and substituting (50) for  $v_R(t)$ , we obtain the following upper bound for  $\dot{V}_2(w(t), \tilde{z}(t), \eta(t))$  of (66) as follows:

$$\dot{V}_2 \leq -k_1 w^2 - k_2 \tilde{z}^T \tilde{z} - k_3 m_2(z, w) \eta^T \bar{M}^{-1} \eta + \left[ \|\eta\| \rho - m_2(z, w) \frac{\eta^T \bar{M}^{-1} \eta \rho^2}{\|\eta\| \rho + \varepsilon_2} \right]. \quad (67)$$

Then by utilizing (45), we note that  $\dot{V}_2(w(t), \tilde{z}(t), \eta(t))$  of (67) can be upper bounded as follows:

$$\dot{V}_2 \leq -\Lambda(w^2 + \tilde{z}^T \tilde{z} + \eta^T \eta) + \left[ \|\eta\| \rho - \frac{\|\eta\|^2 \rho^2}{\|\eta\| \rho + \varepsilon_2} \right] \quad (68)$$

where  $\Lambda \in \mathfrak{R}^1$  is a positive constant defined as

$$\Lambda = \min\{k_1, k_2, k_3\}. \quad (69)$$

After noting that the bracketed term in (68) is less than or equal to  $\varepsilon_2$ , we can use (65) to obtain the following new upper bound for  $\dot{V}_2(w(t), \tilde{z}(t), \eta(t))$ :

$$\dot{V}_2 \leq -2\Lambda V_2 + \varepsilon_2. \quad (70)$$

Standard arguments can now be employed to solve the differential inequality given in (70) as follows:

$$V_2 \leq \exp(-2\Lambda t) V_2(w(0), \tilde{z}(0), \eta(0)) + \frac{\varepsilon_2}{2\Lambda} (1 - \exp(-2\Lambda t)). \quad (71)$$

Finally, we can utilize (65) to obtain the following inequality:

$$\|\Psi_2(w(t), \tilde{z}(t), \eta(t))\| \leq \sqrt{\exp(-2\Lambda t) \|\Psi_2(w(0), \tilde{z}(0), \eta(0))\|^2 + \varepsilon_2 (1 - \exp(-2\Lambda t)) / \Lambda} \quad (72)$$

where the vector  $\Psi_2(w(t), \tilde{z}(t), \eta(t)) \in \mathfrak{R}^5$  is defined as

$$\Psi_2 = [w \quad \tilde{z}^T \quad \eta^T]^T. \quad (73)$$

Based on (72) and (73), it is straightforward to see that  $w(t), \tilde{z}(t), \eta(t) \in \mathcal{L}_\infty$ . After utilizing (13), (21), and the fact that  $\tilde{z}(t), \delta_d(t) \in \mathcal{L}_\infty$ , we can conclude that  $z(t), z_d(t) \in \mathcal{L}_\infty$ . From (15) to (17), the time derivative of (13), (47), (48), (58), (61) we can show that  $u_d(t), u_a(t), \dot{z}_d(t), \dot{\tilde{z}}(t), \dot{z}(t), \dot{w}(t), \Omega_1(t), u(t) \in \mathcal{L}_\infty$ . Now, using standard signal chasing arguments and the development in Appendix A, we can conclude that all of the remaining signals in the control and the system remain bounded during closed-loop operation.

In order to prove (64), we first show that  $z(t)$  defined in (6) goes to a neighbourhood about zero exponentially fast by applying the triangle inequality to (13) to obtain the following bound for  $z(t)$ :

$$\|z\| \leq \|\tilde{z}\| + \|z_d\| \leq \sqrt{\exp(-2\Lambda t) \|\Psi_2(w(0), \tilde{z}(0), \eta(0))\|^2 + \varepsilon_2 (1 - \exp(-2\Lambda t)) / \Lambda} + \alpha_0 \exp(-\alpha_1 t) + \varepsilon_1 \quad (74)$$

where (18), (21), and (72) have been utilized. The GUUB result given by (64) can now be directly obtained from (39), (72)–(74).  $\square$

*Remark 5*

Note that unlike most of the previously proposed tracking controllers (see [6, 13, 15], etc.) we have not imposed any restrictions on the desired trajectory (other than the assumption that  $v_r(t), \dot{v}_r(t), q_r(t)$ , and  $\dot{q}_r(t) \in \mathcal{L}_\infty$ ); hence, the position and orientation tracking problem reduces to the position and orientation regulation problem. That is, if the control objective is targeted at the regulation problem, the desired position and orientation vector, denoted by  $q_r = [x_{rc} \ y_{rc} \ \theta_r]^\top \in \mathbb{R}^3$  and originally defined in (5), becomes an arbitrary desired constant vector. Based on the fact that  $q_r(t)$  is now defined as a constant vector, it is straight forward that  $v_r(t)$  given in (5), and consequently  $f(z, v_r, t)$  defined in (10) equal zero. We also note that the auxiliary variable  $u(t)$  originally defined in (11), is now defined as follows:

$$u = T^{-1}v, \quad v = Tu \quad (75)$$

where the matrix  $T$  was defined in (12). Based on the above simplifications, it is easy to show that the results given by Theorems 1 and 2 are valid for the regulation problem as well.

## 6. EXPERIMENTAL VERIFICATION

### 6.1. Experimental configuration

The proposed robust tracking controller given by (15)–(17), (48), (46), (47) and (50) was implemented on a modified K2A WMR manufactured by Cybermotion Inc. The robot modifications include: (i) the replacement of the pulse-width modulated amplifiers with a dual channel Techron linear amplifier, (ii) the replacement of all existing computational hardware/software with a Pentium 133 MHz PC, and (iii) the replacement of the battery bank with an external power supply. Permanent magnet DC motors provide steering and drive actuation through a 106:1 and a 96:1 gear coupling, respectively. The positions of the steering and drive motors are measured via Hewlett Packard (HEDS-9000) encoders with a resolution of 0.35°/line, and velocity measurements were calculated via a filtered backwards difference algorithm. A Pentium 133 MHz PC operating under QNX (a real-time micro-kernel-based operating system) hosts the control algorithm that was written in 'C', and implemented using Qmotor 2.0 (an in-house graphical user interface). Data acquisition and control implementation were performed at a frequency of 2.0 kHz using the MultiQ I/O board. In order to measure the tracking error given in (7) we need to determine the  $x(t)$  and  $y(t)$  co-ordinate and the orientation of the WMR. To this end, we obtained the positions of the steering and drive motors via the aforementioned encoders, and then calculated the linear and angular velocity measurements via a filtered backwards difference algorithm. Using the angular position measurement and the linear and angular velocity measurements, we were able to utilize the relationship given in (1) to determine  $\dot{x}(t)$  and  $\dot{y}(t)$ . We were then able to use a trapezoidal integration routine with (1) to obtain the actual values of the Cartesian co-ordinates of the WMR. For simplicity the electrical dynamics of the system were ignored. That is, we assume that the computed torque is statically related to the voltage input of the permanent magnet DC motors by a constant.

### 6.2. Experimental results

The dynamics for the modified K2A WMR are given as follows:

$$\frac{1}{r_0} \begin{bmatrix} 1 & 0 \\ 0 & \frac{L_0}{2} \end{bmatrix} \begin{bmatrix} \tau_1 \\ \tau_2 \end{bmatrix} = \begin{bmatrix} m_0 & 0 \\ 0 & I_0 \end{bmatrix} \begin{bmatrix} \dot{v}_1 \\ \dot{v}_2 \end{bmatrix} + \begin{bmatrix} F_{s1} & 0 \\ 0 & F_{s2} \end{bmatrix} \begin{bmatrix} \text{sgn}(v_1) \\ \text{sgn}(v_2) \end{bmatrix} + \begin{bmatrix} F_{d1} & 0 \\ 0 & F_{d2} \end{bmatrix} \begin{bmatrix} v_1 \\ v_2 \end{bmatrix} \quad (76)$$

where  $m_0 = 165$  kg denotes the mass of the robot,  $I_0 = 4.643$  kg m<sup>2</sup> denotes the inertia of the robot,  $r_0 = 0.010$  m denotes the radius of the wheels,  $L_0 = 0.667$  m denotes the length of the axis between the wheels, and the dynamic and static friction elements are denoted by  $F_{s1}$ ,  $F_{s2}$ ,  $F_{d1}$ , and  $F_{d2}$ . The desired reference linear and angular velocity were selected as

$$v_{r1} = 0.2 \text{ (m/s)} \quad v_{r2} = 0.4 \sin(0.5t) \text{ (rad/s)} \quad (77)$$

respectively, (see Figure 1 for the resulting reference time-varying Cartesian position and orientation).

The Cartesian positions and the orientation were initialized to zero, and the auxiliary signal  $z_d(t)$  was initialized as follows:

$$z_d(0) = [0.01 \ 0.01]^T. \quad (78)$$

The best guess estimates for the mass and inertia of the WMR were selected to be 50 per cent of the actual values in order to calculate the feedforward term  $\hat{\kappa}(\cdot)$  given in (53) (note that the static and dynamic friction components were assumed to be included in the bounded disturbance term  $T_d$  given in (41)). For simplicity, the bounding function  $\rho(\eta, w, z_d, z, t)$  given in (51) was selected as  $\rho = 0.5$ . The control gains that resulted in the best performance are given below

$$k_1 = 55.5, \quad k_2 = 65.0, \quad k_3 = \begin{bmatrix} 0.65 & 0 \\ 0 & 16.0 \end{bmatrix} \quad (79)$$

$$\alpha_0 = 0.014, \quad \alpha_1 = 27.5, \quad \varepsilon_1 = 1.0, \quad \varepsilon_2 = 0.75.$$

Note that although  $k_3$  of (46) was defined as a scalar constant, we used the values given in (79) to facilitate the 'tuning' process. The position/orientation tracking error of the COM of the WMR and the associated control torque inputs are shown in Figures 2–4, respectively (note the control torque inputs plotted in Figure 4 represent the torques applied after the gearing mechanism). Based on Figures 2 and 3, it is clear that the steady-state position/orientation tracking error is bounded as follows:

$$|\tilde{x}| < 8 \text{ mm}, \quad |\tilde{y}| < 11 \text{ mm}, \quad |\tilde{\theta}| < 0.85^\circ \quad (80)$$

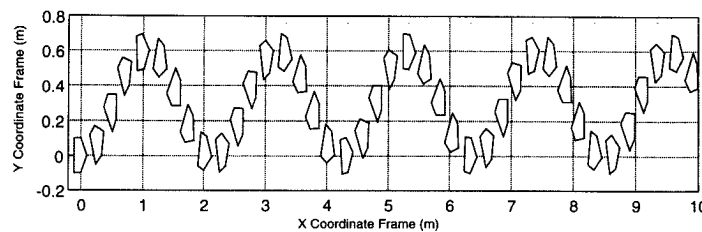


Figure 1. Desired cartesian trajectory.

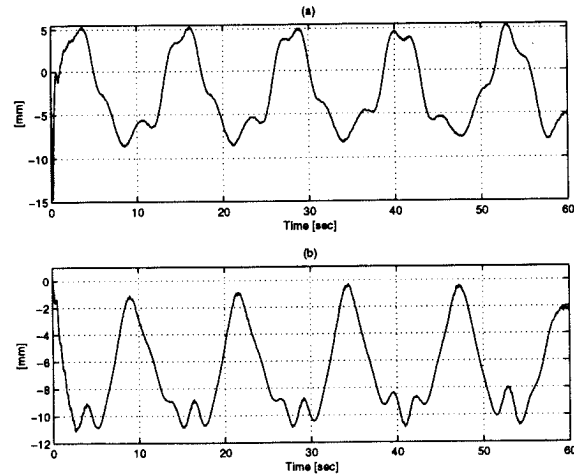


Figure 2. Position tracking error: (a)  $\tilde{x}$  and (b)  $\tilde{y}$ .

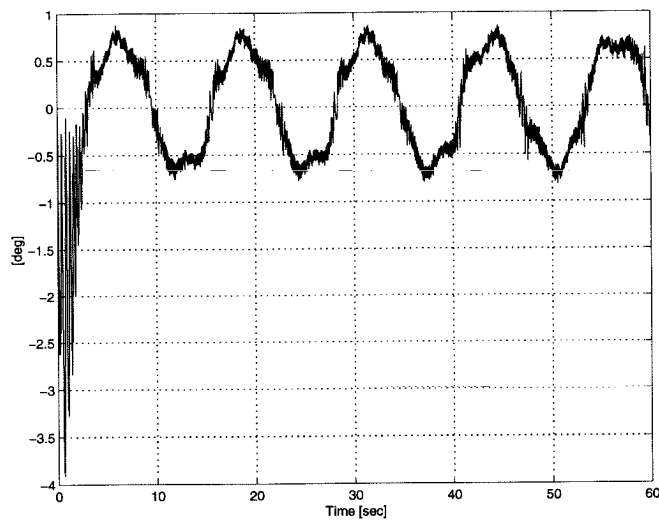


Figure 3. Orientation tracking error  $\tilde{\theta}$ .

*Remark 6*

The control gain values used in (79) were found as a result of ‘tuning’ the controller until the position/orientation tracking error improved. Note that similar results may be obtained by ‘tuning’ the controller in a slightly different manner.

*Remark 7*

Due to unmodeled effects associated with the wheels and the drive mechanism (i.e. slippage, backlash, etc.), it is impossible to determine the actual position/orientation tracking errors of the WMR since we must rely solely on position measurements from the encoders. An additional

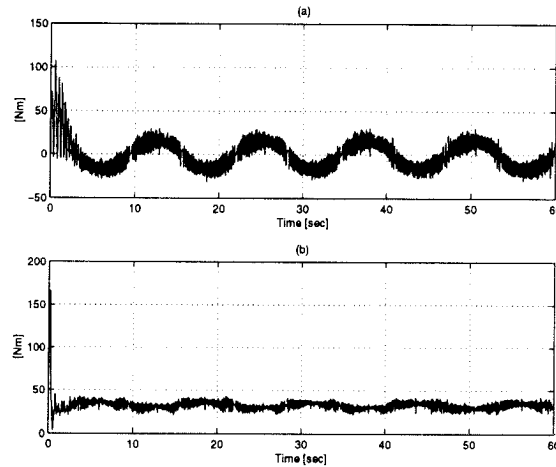


Figure 4. Control torque input: (a) steering motor and (b) drive motor.

problem that is associated with the K2A mobile robot is that the encoder that provides angular position measurements is mounted after the gearing mechanism. Hence, the placement of the low-resolution angular position encoder after the gearing mechanism results in the problem that the motor must turn  $37.27^\circ$  before any motion is detected. Since, the angular position measurement is required for calculating both the position and orientation signals (see the discussion in the experimental configuration section), we believe that the initial chattering observed in Figure 3 and the 'shift' in the  $y$ -coordinate tracking error in Figure 2 could be associated with the aforementioned concerns. In addition, we believe that if encoders having a higher resolution could somehow be mounted before the gearing mechanism then the tracking error bounds given in (80) could be decreased further.

## 7. CONCLUSION

In this paper, we have presented the design of a robust nonlinear tracking controller for a mobile robot system. Through the use of a Lyapunov-based stability analysis, we have demonstrated that: (i) the position and orientation tracking errors globally exponentially converge to a neighbourhood about zero that can be made arbitrarily small, (ii) the controller provides robustness with regard to parametric uncertainty and additive bounded disturbances in the dynamic model, and (iii) a unified scheme was developed which solves both the tracking and the regulation problems. In addition to the WMR problem, the proposed kinematic controller can be applied to other non-holonomic systems (see [5] for examples), and hence, its applicability extends farther than the mobile robot problem. Experimental trials on a modified Cybermotion K2A mobile robot system were used to illustrate the feasibility and the performance of the proposed controller. Future work will involve the redesign of the proposed kinematic controller to allow it to be used in the design of an adaptive controller for the compensation of uncertainty in the dynamic model.<sup>§</sup>

<sup>§</sup>For several technical reasons associated with the structure of the transformed system given by (8), it is not obvious how one can redesign the proposed kinematic controller to achieve this objective.



## APPENDIX A

To calculate  $\dot{u}_d(t)$ , we take the time derivative of (48), substitute for the time derivative of  $u_d(t)$  defined in (15), utilize (8) and then add and subtract  $k_2 u_d$  to the left-hand side to obtain

$$\dot{u}_d = \left( \frac{k_1 \dot{w} + \dot{f}}{\delta_d^2} \right) J z_d - 2 \left( \frac{(k_1 w + f) \dot{\delta}_d}{\delta_d^3} \right) J z_d + \dot{\Omega}_1 z_d + \left( \Omega_1 + \left( \frac{k_1 w + f}{\delta_d^2} \right) J \right) \dot{z}_d - k_2 [u_d - \eta]. \quad (\text{A1})$$

Second, to illustrate that  $\dot{u}_d(t) \in \mathcal{L}_\infty$ , we utilize (48), (15)–(17), (26), (9), (13), (18), (21), the time derivative of  $\Omega_1(t)$ , and the fact that

$$|\dot{f}| \leq 4 \|v_r\| (\|\dot{z}_d\| + \|\dot{\tilde{z}}\|) + 4 \|\dot{v}_r\| (\|z_d\| + \|\tilde{z}\|) \quad (\text{A2})$$

to upper bound  $\dot{u}_d(t)$  as follows:

$$\begin{aligned} \dot{u}_d &\leq \left( \frac{k_1 \dot{w}}{\delta_d^2} \right) J z_d + \left( \frac{4 \|v_r\| (\|\dot{z}_d\| + \|\dot{\tilde{z}}\|) + 4 \|\dot{v}_r\| (\|z_d\| + \|\tilde{z}\|)}{\delta_d^2} \right) J z_d \\ &\quad - 2 \left( \frac{(k_1 w + f) \dot{\delta}_d}{\delta_d^3} \right) J z_d + \frac{\ddot{\delta}_d}{\delta_d} z_d - \frac{\dot{\delta}_d^2}{\delta_d^2} z_d + \frac{(2k_1 w + f) \dot{w}}{\delta_d^2} z_d \\ &\quad + \frac{w(4 \|v_r\| (\|\dot{z}_d\| + \|\dot{\tilde{z}}\|) + 4 \|\dot{v}_r\| (\|z_d\| + \|\tilde{z}\|))}{\delta_d^2} z_d \\ &\quad - 2 \left( \frac{(k_1 w^2 + wf) \dot{\delta}_d}{\delta_d^3} \right) z_d + \left( \Omega_1 + \left( \frac{k_1 w + f}{\delta_d^2} \right) J \right) \dot{z}_d - k_2 [u_d - \eta]. \quad (\text{A3}) \end{aligned}$$

Thus, based on the definition of  $\delta_d(t)$  given in (18) and the fact that  $\dot{w}$ ,  $\dot{\tilde{z}}$ ,  $\dot{z}_d$ ,  $v_r$ ,  $\dot{v}_r$ ,  $w$ ,  $f$ ,  $z_d$ ,  $\tilde{z}$ ,  $u_d$ ,  $\eta \in \mathcal{L}_\infty$  (see Theorem 2), it is straightforward to see from (A3) that  $\dot{u}_d(t) \in \mathcal{L}_\infty$ .

## REFERENCES

1. Canudas de Wit C, Khennoufc K, Samson C, Sordalen OJ. Nonlinear control for mobile robots. *Recent Trends in Mobile Robots*, Zheng Y. (ed.). World Scientific: New Jersey, 1993.
2. Brockett R. Asymptotic stability and feedback stabilization. In *Differential Geometric Control Theory*, Brockett R, Millman R, Sussmann H. (eds). Birkhauser: Boston, 1983.
3. McCloskey R, Murray R. Exponential stabilization of driftless nonlinear control systems using homogeneous feedback. *IEEE Transactions on Automatic Control* 1997; **42**(5):614–628.
4. Samson C. Velocity and torque feedback control of a nonholonomic cart. *Proceedings of the International Workshop in Adaptive and Nonlinear Control: Issues in Robotics*, Grenoble, France, 1990.
5. Bloch A, Reyhanoglu M, McClamroch N. Control and stabilization of nonholonomic dynamic systems. *IEEE Transactions on Automatic Control* 1992; **37**(11).
6. Canudas de Wit C, Sordalen O. Exponential stabilization of mobile robots with nonholonomic constraints. *IEEE Transactions on Automatic Control* 1992; **37**(11):1791–1797.
7. Coron J, Pomet J. A remark on the design of time-varying stabilizing feedback laws for controllable systems without drift. In *Proceedings of the IFAC Symposium on Nonlinear Control Systems Design (NOLCOS)*, Bordeaux, France, June 1992; 413–417.
8. Pomet J. Explicit design of time-varying stabilizing control laws for a class of controllable systems without drift. *Systems Control Letters* 1992; **18**(2):147–158.
9. Teel A, Murray R, Walsh C. Non-holonomic control systems: from steering to stabilization with sinusoids. *International Journal Control* 1995; **62**(4):849–870.
10. Jiang Z. Iterative design of time-varying stabilizers for multi-input systems in chained form. *Systems Control Letters* 1996; **28**:255–262.

11. Samson C. Control of chained systems application to path following and time-varying point-stabilization of mobile robots. *IEEE Transactions on Automatic Control* 1997; **40**(1):64–77.
12. Godhavn J, Egeland O. A Lyapunov approach to exponential stabilization of nonholonomic systems in power form. *IEEE Transactions on Automatic Control* 1997; **42**(7):1028–1032.
13. Kanayama Y, Kimura Y, Miyazaki F, Noguchi T. A stable tracking control method for an autonomous mobile robot. *Proceedings of the IEEE International Conference on Robotics and Automation* 1990; 384–389.
14. Walsh G, Tilbury D, Sastry S, Murray R, Laumond JP. Stabilization of trajectories for systems with nonholonomic constraints. *IEEE Transactions on Automatic Control* 1994; **39**(1):216–222.
15. Jiang Z, Nijmeijer H. Tracking control of mobile robots: a case study in backstepping. *Automatica* 1997; **33**(7):1393–1399.
16. Jiang Z, Nijmeijer H. A recursive technique for tracking control of nonholonomic systems in the chained form. *IEEE Transactions on Automatic Control* 1999; **44**(2):265–279.
17. Escobar G, Ortega R, Reyhanoglu M. Regulation and tracking of the nonholonomic double integrator: a field-oriented control approach. *Automatica* 1998; **34**(1):125–131.
18. Dong W, Huo W. Adaptive stabilization of dynamic nonholonomic chained systems with uncertainty. *Proceedings of the 36th IEEE Conference on Decision and Control*, December 1997; 2362–2367.
19. Aguilar LE, Soueres P, Courdresses M, Fleury S. Robust path-following control with exponential stability for mobile robots. *Proceedings of the IEEE International Conference on Robotics and Automation* 1998; 3279–3284.
20. Corless M, Leitman G. Continuous state feedback guaranteeing uniform ultimate boundedness for uncertain dynamic systems. *IEEE Transactions on Automatic Controls* 1981; **AC-26**(5):1139–1143.
21. Lewis F, Abdallah C, Dawson D. *Control of Robot Manipulators*. Macmillan: New York, 1993.